AGU PUBLICATIONS

Geophysical Research Letters

RESEARCH LETTER
10.1002/2014GL061432

Key Points:
- Thermomagnetic stability of nonideal magnetite particles
- Visualization of stability of vortex domain state with heating
- Particles behave like uniaxial SD particles near to Curie temperature

Correspondence to:
T. P. Almeida,
t.almeida@imperial.ac.uk

Citation:
Almeida, T. P., T. Kasama, A. R. Muxworthy, W. Williams, L. Nagy, and R. E. Dunin-Borkowski (2014), Observing thermomagnetic stability of nonideal magnetite particles: Good paleomagnetic recorders?, *Geophys. Res. Lett.*, *41*, 7041–7047, doi:10.1002/2014GL061432.

Received 6 AUG 2014
Accepted 19 SEP 2014
Accepted article online 23 SEP 2014
Published online 17 OCT 2014

Observing thermomagnetic stability of nonideal magnetite particles: Good paleomagnetic recorders?

Trevor P. Almeida[1], Takeshi Kasama[2], Adrian R. Muxworthy[1], Wyn Williams[3], Lesleis Nagy[3], and Rafal E. Dunin-Borkowski[4]

[1]Department of Earth Science and Engineering, Imperial College London, London, UK, [2]Center for Electron Nanoscopy, Technical University of Denmark, Kongens Lyngby, Denmark, [3]School of GeoSciences, University of Edinburgh, Edinburgh, UK, [4]Ernst Ruska-Centre for Microscopy and Spectroscopy with Electrons and Peter Grünberg Institute, Forschungszentrum Jülich, Jülich, Germany

Abstract The thermomagnetic behavior of remanence-induced magnetite (Fe_3O_4) particles in the pseudo-single-domain (PSD) size range (~0.1–10 μm), which dominate the magnetic signature of many rock lithologies, is investigated using off-axis electron holography. Construction of magnetic induction maps allowed for the visualization of the vortex domain state in an individual Fe_3O_4 grain (~200 nm in diameter) as a function of temperature. Acquisition of a series of electron holograms at 100°C intervals during in situ heating up to 700°C demonstrates the vortex state of the Fe_3O_4 grain, in this instance, remains thermally stable close to its unblocking temperature and exhibits a similar in-plane remanent state upon cooling; i.e., the particle is effectively behaving like a uniaxial single-domain particle to temperatures near T_C. Such particles are thought to be robust magnetic recorders. It is suggested that evidence for PSD behavior should therefore not preclude paleomagnetic investigation.

1. Introduction

Magnetic minerals in rocks record the direction and intensity of the ambient magnetic field during formation, providing, for example, information on the geomagnetic field variation and past tectonic plate motions. The primary form of natural remanent magnetization in igneous rocks is thermoremanent magnetization (TRM) and is acquired by the constituent magnetic minerals on cooling from the Curie temperature (T_C (~580°C for magnetite)). *Néel*'s [1949, 1955] TRM theories have been shown to describe the behavior of the smallest magnetically uniform grains (single domain (SD)); however, most rocks contain larger magnetic grains that display nonuniform magnetic structures (multidomain (MD)). The magnetic signature in igneous rocks is usually dominated by small MD grains (~0.1–10 μm), often termed pseudo-single-domain (PSD), as their bulk magnetic characteristics are similar, but not identical, to SD particles. However, there is currently no physical model for PSD TRM acquisition. To construct such model, a numerical algorithm that includes computationally intensive thermal fluctuations is needed. Verification of the numerical predictions through direct observations of the magnetization in submicron grains (<500 nm) at temperature is therefore also required. Both of these aspects are challenging and have not yet been unambiguously resolved, although advances have been made numerically [*Thomson et al.*, 1994; *Winklhofer et al.*, 1997; *Muxworthy et al.*, 2003] and experimentally [*Metcalf and Fuller*, 1988; *de Groot*, 2013].

The transmission electron microscopy (TEM) technique of off-axis electron holography permits the nanometer-scale imaging of magnetic induction within and around materials as a function of applied field and temperature [*Dunin-Borkowski et al.*, 1998; *Kasama et al.*, 2010, 2013]. This is the only technique that can produce high-resolution images of magnetic domain states in nanometric grains. It has been applied in mineral magnetism for more than a decade [*Harrison et al.*, 2002; *Bryson et al.*, 2014; *Almeida et al.*, 2014] but has not previously been used to examine thermal behavior above room temperature.

To help advance our understanding, in this paper, the first use of off-axis electron holography to examine local changes in remanent magnetization in a PSD magnetite grain during in situ heating is reported. We observe the evolution of the remanent domain structure of an individual synthetic magnetite grain

induced with a room temperature saturation isothermal remanence (SIRM), as it is heated to ~700°C and subsequently cooled to room temperature. The observations are complemented by bulk magnetic measurements at room temperature and above.

2. Experiment

Fe_3O_4 particles with a diameter ranging from ~150 nm to ~250 nm (hydrothermally synthesized by Nanostructured and Amorphous Materials, USA) were cleaned with acetone and centrifuged for 6 min at 6000 rpm. The Fe_3O_4 particles were deposited onto single crystal silicon substrates for crystallographic identification using X-ray diffractometry (PANalytical X'Pert PRO Diffractometer). For the purpose of in situ heating TEM investigations, the particles were dispersed in distilled water using an ultrasonic bath before deposition onto Aduro E-chip TEM sample holder (Protochips, USA). The sample was preheated in situ in the TEM to 700°C for the purpose of evaporating the remaining water and alleviate possible strain induced during particle synthesis. Off-axis electron holograms were acquired at 300 kV in Lorentz mode in a Titan 80–300 TEM with a charge-coupled device camera and an electron biprism operated typically at 160 V (Center for Electron Nanoscopy, Technical University of Denmark). The direction of magnetization in the particle was initially reversed at room temperature in situ in the TEM by tilting the sample by ±30° and turning on the conventional microscope objective lens to apply a magnetic field of 2 T to the sample, parallel to the direction of the electron beam. The objective lens was then turned off and the sample tilted back to 0° for hologram acquisition in field-free conditions (residue field is $<$0.2 mT) with the particles induced with a room temperature SIRM. The different holograms were recorded with the particle magnetized in opposite directions, and the mean inner potential was separated from the magnetic potential, as described by *Dunin-Borkowski et al.* [1998]. Electron holograms were then acquired in field-free conditions during in situ heating at 100°C intervals from 100°C up to 700°C at 1°C/s using a Protochips heating holder (as displayed on the Protochips temperature control) and again upon cooling, where the acquisition time was 4 s. The mean inner potential was subtracted from the unwrapped total phase shift, acquired at each temperature interval, to allow the construction of magnetic induction maps representative of the magnetic remanence. In this paper, the temperatures are all nominal as the absolute temperature of the particle itself is not accurately known. To complement the experimental work, a micromagnetic model containing unstructured meshes was used to simulate a magnetic induction map. The meshed grain geometry was based on two-dimensional information acquired from the bright-field TEM image (Figure 2a). Micromagnetic solutions of the domain structure were calculated for the particle from an initial saturated state parallel to the saturation field of 2 T, as applied during the acquisition of the holography images. Equilibrium magnetic structure solutions were then used to calculate the magnetic vector potential $\boldsymbol{A}$. Once $\boldsymbol{A}$ was known, the phase shift was computed by integrating the component of $\boldsymbol{A}$ perpendicular to the plane of the TEM image of Figure 2a ($\boldsymbol{A}_z$) according to equation

$$H^{ij} = \cos\left(c\sum_{k=1}^{n}\boldsymbol{A}_z^{ijk}\right)$$

where c represents a phase amplification factor. The contours of H^{ij} were then colored according to the planar magnetic flux density $\boldsymbol{B}$. For the purpose of bulk magnetic measurements, the Fe_3O_4 powder was dispersed in a cement/curing agent mixture and, once dried, examined at the paleomagnetic laboratory at Imperial College London. The focus of this experimental work was observational, and hence, the interparticle spacing was not controlled tightly during sample preparation. Room temperature, first-order reversal curve (FORC), and high-temperature thermomagnetic measurements were performed using a Princeton Measurements Vibrating Sample Magnetometer, fitted with a furnace, with heating performed in flowing He. To replicate the TEM experiments, the thermomagnetic experiment was initially performed to alleviate possible strain induced during synthesis of the particles, and the data were acquired from the second measurement.

3. Results

Figure 1 provides information on the general crystallography, size, morphology, and bulk magnetic properties of the Fe_3O_4 nanoparticles (NPs). The peaks in the X-ray diffraction (XRD) pattern of Figure 1a are in excellent agreement with the presence of stoichiometric Fe_3O_4 (JCPDS 75-449). The bright-field image

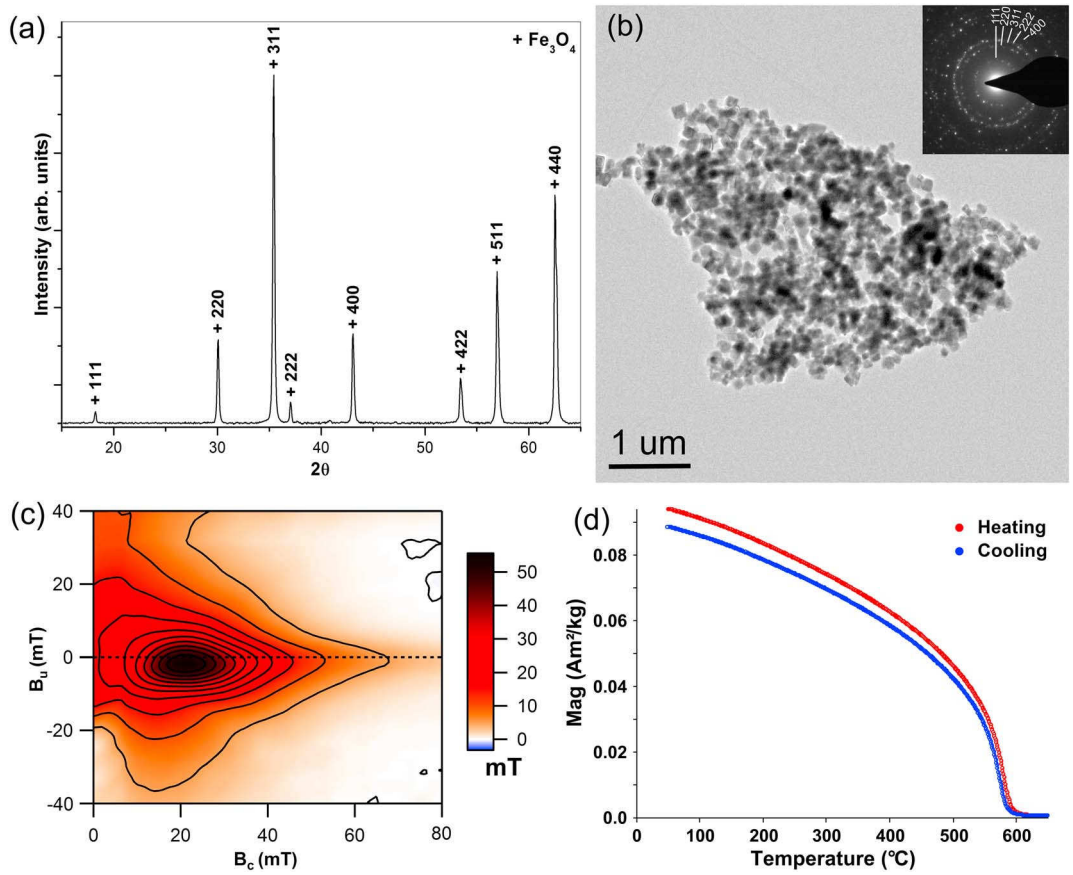

Figure 1. General crystallography, size, morphology, and bulk magnetic properties of the Fe_3O_4 particles. (a) XRD pattern of the NPs, confirming the Fe_3O_4 phase (indexed, JCPDS 75-449). (b) Bright-field TEM image of the Fe_3O_4 particles (150–250 nm in diameter) with associated SAED patterns indexed to Fe_3O_4 (JCPDS 75-449). (c) FORC diagram acquired at room temperature (smoothing factor = 4). The measurement time was 250 ms. (d) Thermomagnetic curves of the Fe_3O_4 particles. Heating was performed in flowing helium, in a field of 300 mT.

of Figure 1b displays generally isotropic, facetted grains in the size range of ~150 nm to ~250 nm, with selected area electron diffraction (SAED) (Figure 1b, inset) confirming the assignment of Fe_3O_4. The FORC diagram of Figure 1c displayed PSD/SD-type behavior with a distinct peak [*Muxworthy and Dunlop*, 2002]. High-temperature thermomagnetic analysis (Figure 1d) indicated that the Fe_3O_4 NPs were thermally stable. The T_C was determined from the heating curve using the second-derivative method [*Tauxe*, 1998] and calculated as 585 ± 5°C, which is in good agreement with stoichiometric magnetite.

The bright-field TEM image of Figure 2a shows a smooth-surfaced Fe_3O_4 grain (~200 nm in diameter), as confirmed by SAED (Figure 2a, inset). Figures 2b–2p depict the effect of heating and cooling on the room temperature SIRM in the same grain, visualized through construction of a series of magnetic induction maps. The initial magnetic induction map (Figure 2b) contains evenly spaced magnetic contours, spanning from the surface to the center of the grain, flowing in a counterclockwise direction (denoted by arrows), and is indicative of a vortex state. The magnetic induction maps of Figures 2c–2i demonstrate the effect of increasing temperature from 100°C to 700°C, where widening of the phase contours within the Fe_3O_4 grain is indicative of a reduction in the remanent magnetic field. Likewise, the magnetic induction maps of Figures 2i–2p show the effect of cooling from 700°C to room temperature; narrowing of the magnetic contours during cooling demonstrates the recovery of the remanent magnetic field, similar to the initial remanence exhibited prior to heating. The existence of the remanent magnetization at 700°C (Figure 2i) is likely a discrepancy; i.e., the absolute T_C is <600°C and is considered in the Discussion section.

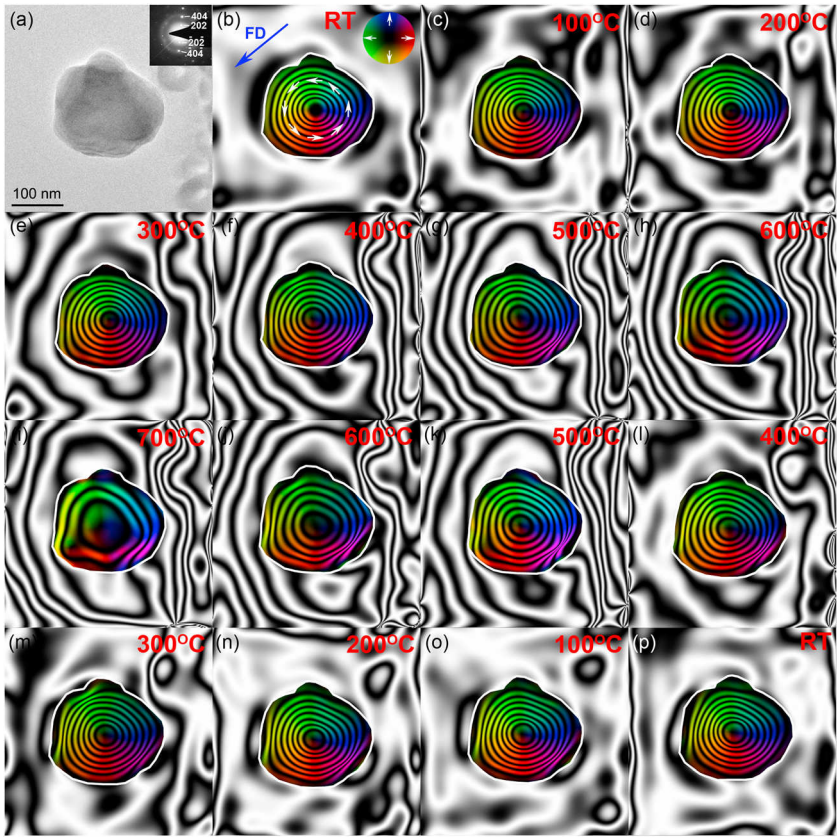

Figure 2. Visualization of the effect of nominal temperature on the magnetic domain state of an individual Fe_3O_4 grain. (a) Bright-field TEM image of the Fe_3O_4 particle (~200 nm in diameter) with SAED pattern (inset) indexed to Fe_3O_4 (JCPDS 75-449). Magnetic induction maps reconstructed from holograms taken at (b) room temperature (with the arrow, labeled FD, showing direction of the applied saturating field to induce magnetic remanence) and during in situ heating to (c) 100°C, (d) 200°C, (e) 300°C, (f) 400°C, (g) 500°C, (h) 600°C, and (i) 700°C, as well as upon subsequent cooling to (j) 600°C, (k) 500°C, (l) 400°C, (m) 300°C, (n) 200°C, (o) 100°C, and (p) room temperature. The contour spacing is 0.79 rad.

By way of supporting information, the micromagnetic model of Figure 3a provides a 3-D representation of the magnetic domain structure in the Fe_3O_4 grain, presented in Figure 2. Figure 3b shows the model to exhibit central magnetic moments of vortex flowing in a counterclockwise direction. The associated holography simulation of Figure 3c, derived from the model in Figure 3a, presents evenly spaced magnetic contours, spanning from the surface to the center of the grain, flowing in a counterclockwise direction (denoted by arrows), in a similar manner to the experimentally acquired magnetic induction map (Figure 2b). Figures 3d–3f present data acquired from the contribution to the total phase shift after the mean inner potential, acquired at room temperature, is subtracted and used to construct magnetic induction maps (Figure 2). The room temperature phase image is shown in Figure 3d, and selected line profiles taken along the center of the Fe_3O_4 grain are plotted in Figure 3e. The reduction in the amplitude of the phase shift with heating from room temperature is indicative of a loss in magnetic remanence, which is then seen to recover upon cooling. Figure 3f shows the variation of amplitude of the phase shift with temperature across the entire temperature range during both heating and cooling. There is a steady decrease in the amplitude of the phase shift from room temperature to 700°C and a subsequent recovery on cooling, which exhibits almost a near linear trend with nominal temperature.

4. Discussion

The FORC data are consistent with the magnetic behavior of PSD Fe_3O_4, complemented by a thermomagnetic curve displaying a T_C characteristic of stoichiometric magnetite. The magnetic induction map of the

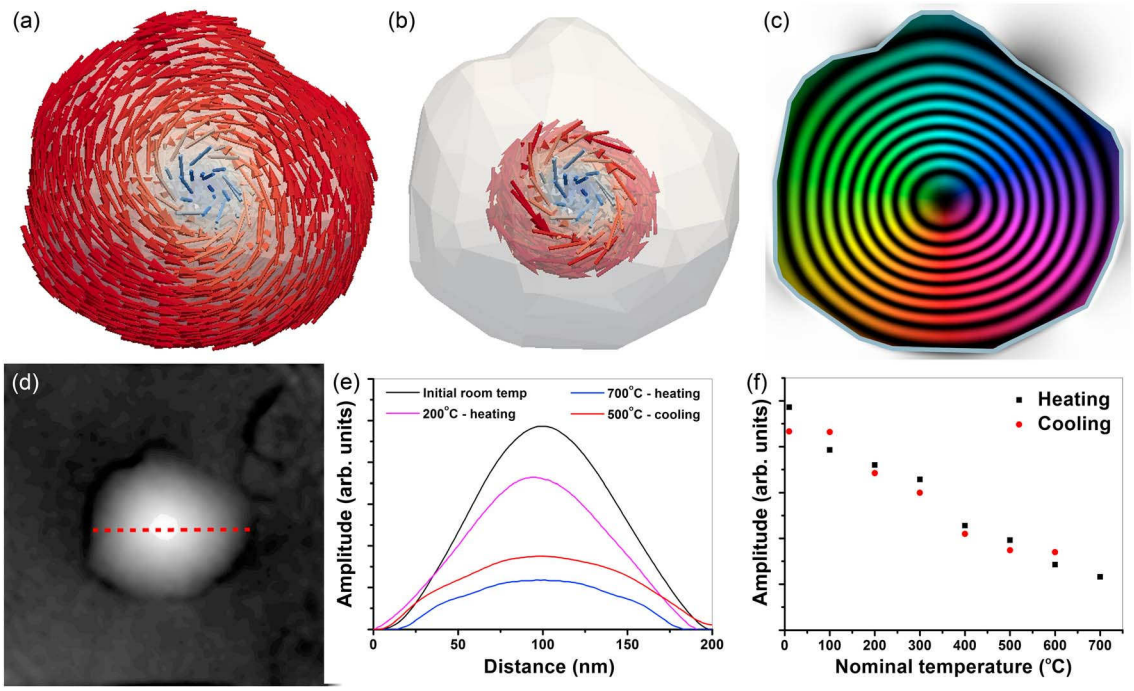

Figure 3. (a and b) Micromagnetic modeling of the Fe_3O_4 grain showing (Figure 3a) magnetic moments flowing counterclockwise around (Figure 3b) a central vortex and the (c) associated simulated magnetic induction map. (d-f) Contribution to the total phase shift after the mean inner potential, acquired at room temperature, is subtracted (used to construct the magnetic induction maps in Figure 2). (d) Example of the magnetic contribution to phase image (room temperature) and (e) selected line profiles across the center of the Fe_3O_4 grain in the phase image (dashed line in Figure 3d) taken at room temperature, 200°C and 700°C during heating and 500°C upon cooling. (f) Plot showing the relationship between amplitudes of the phase shift and nominal temperature.

~200 nm Fe_3O_4 grain (Figure 2b) acquired at room temperature clearly shows that the SIRM is carried by a vortex domain state structure. The associated simulated magnetic induction map is near identical to the experimentally acquired induction map, thereby validating the 3-D model of a magnetic vortex, and hence, the Fe_3O_4 grain exhibits an ideal PSD state for investigating the thermal stability of nonideal recorders. The overall structure is seen to be essentially stable to thermal effects, with widening of the phase contours as a consequence of increasing temperature to 700°C, suggestive of a reduction in total remanent magnetization, which is further emphasized by the decrease in phase amplitude with temperature (Figure 3f). It is recognized that 700°C is significantly higher than the T_C of Fe_3O_4, and hence, no remanent magnetization would be expected. Thermomagnetic analysis (Figure 1d) indicates that this discrepancy lies with the acquired TEM data and is considered to have two contributing factors: First, slight electrostatic charging of both the SiN supporting membrane and the Fe_3O_4 grain with temperature is likely to result in a net contribution after the room temperature mean inner potential is subtracted from the total phase shift [*Beleggia and Pozzi*, 2010]. This effect is emphasized by the development of a stray field, seen to be most prominent from 300 to 700°C on heating, in addition to 600°C and 500°C upon cooling. Second, the mean inner potential of the Fe_3O_4 grain itself may change slightly with increasing temperature due to an associated variation in electrical conductivity [*Kamilov et al.*, 1975], alongside a possible contribution from thermal expansion [*Manahan*, 1990]. Acquiring the mean inner potential contribution to total phase shift at each temperature interval, in a separate experiment, and then subtracting it from the phase shift, acquired at remanence, could remove this effect in the future. Nevertheless, the relatively linear decrease in the amplitude of the phase shift with increasing nominal temperature up to 700°C is consistent with the thermal behavior of Fe_3O_4 particles. Subsequent narrowing of the phase contours and associated increase of amplitude upon cooling are representatives of a recovery in magnetic remanence strength.

The direction of the vortex core is unknown, as it lies normal to the plane of this ~200 nm Fe_3O_4 grain; i.e., the core moment aligns either in or out of plane. However, the key finding of this study is that the

vortex structure is essentially stable during heating to temperatures close to the T_C. As the core moment only aligns in one of the two orientations, this effectively means that the particle is behaving like a uniaxial single-domain particle to temperatures near T_C. Such particles found the basis of most TRM models and are thought to be robust magnetic recorders.

It is recognized that there is a spurious addition to the phase shift at elevated temperatures, and hence, the phase shifts do not exclusively represent the magnetic contribution, and work must be done to reduce this effect in the future. Nevertheless, this is the first experiment showing the magnetic remanence of individual nanoscale PSD grains, which dominate the magnetic signal in rocks, as a function of temperature.

While rocks containing such domain structures would not usually be thought of as being ideal paleomagnetic recorders (although their FORC diagram might indicate otherwise), the image sequence (Figure 2) suggests that they will accurately record both in-plane paleodirection and paleointensity information, and are stable under heating to relatively high temperatures. This finding directly and visually supports recent thermomagnetic work, including Thellier-type paleointensity study, on synthetic magnetite samples produced by electron beam lithography [*Muxworthy et al*., 2014]. *Muxworthy et al.* [2014] found that arrays of near-identical PSD particles with controlled intergrain spacing were reliable recorders of a weak-field thermoremanence, from which accurate paleointensities could be recovered using a Thellier-type protocol [e.g., *Tauxe and Yamazaki*, 2007]. The effect of multiple repeat heatings as used in typical paleointensity investigations has yet to be investigated using electron holography.

5. Conclusions

Construction of the magnetic induction maps acquired from a vortex magnetic structure in an ~200 nm grain of PSD magnetite as a function of temperature indicates that its magnetic remanence is stable to heating to near its T_C. These direct observations visually demonstrate, for the first time, the SD-like stability of small MD, magnetite grains. These findings imply that structures that initially appear to be a nonideal magnetic recorder are in fact likely to reliably record both paleodirectional and paleointensity information. As a large percentage of rocks appear to be magnetically dominated by PSD grains that contain vortex-like magnetic states (Figure 2), it is suggested that evidence for PSD behavior should not preclude paleomagnetic investigation.

Acknowledgments

The authors would like to thank the Natural Environment Research Council for funding NERC grant NE/H00534X/1. Thanks also go to the Center for Electron Nanoscopy at the Technical University of Denmark for the use of their microscopy facilities. The data for this paper are available at NERC-designated data center for the Earth Sciences, the National Geoscience Data Centre.

Michael Wysession thanks Richard Harrison and one anonymous reviewer for their assistance in evaluating this paper.

References

Almeida, T. P., A. R. Muxworthy, W. Williams, T. Kasama, and R. E. Dunin-Borkowski (2014), Magnetic characterization of synthetic titanomagnetites: Quantifying the recording fidelity of ideal synthetic analogs, *Geochem. Geophys. Geosyst.*, *15*, 161–175, doi:10.1002/2013GC005047.

Beleggia, M., and G. Pozzi (2010), Phase shift of charged metallic nanoparticles, *Ultramicroscopy*, *110*, 418–424.

Bryson, J. F. J., N. S. Church, T. Kasama, and R. J. Harrison (2014), Nanomagnetic intergrowths in Fe–Ni meteoritic metal: The potential for time-resolved records of planetesimal dynamo fields, *Earth Planet. Sci. Lett.*, *388*, 237–248.

de Groot, L. V. (2013), *High-Resolution Records of Non-Dipole Variations in the Intensity of the Earth's Magnetic Field*, Utrecht Stud. in Earth Sci., PhD thesis, vol. 37, Utrecht Univ., Utrecht, Netherlands.

Dunin-Borkowski, R. E., M. R. McCartney, R. B. Frankel, D. A. Bazylinski, M. Pósfai, and P. R. Buseck (1998), Magnetic microstructure of magnetotactic bacteria by electron holography, *Science*, *282*, 1868–1870.

Harrison, R. J., R. E. Dunin-Borkowski, and A. Putnis (2002), Direct imaging of nanoscale magnetic interactions in minerals, *Proc. Natl. Acad. Sci. U.S.A.*, *99*, 16,556–16,561.

Kamilov, I. K., G. M. Shakhshaev, K. K. Aliev, G. G. Musaev, and M. M. Khamidov (1975), Some features of the behavior of the thermal conductivity of ferrites in the vicinity of magnetic phase transitions, *J. Exp. Theor. Phys.*, *41*(2), 290–296.

Kasama, T., N. Church, J. M. Feinberg, R. E. Dunin-Borkowski, and R. J. Harrison (2010), Direct observation of ferromagnetic/ferroelastic domain interactions in magnetite below the Verwey transition, *Earth Planet. Sci. Lett.*, *297*, 10–17.

Kasama, T., R. J. Harrison, N. S. Church, M. Nagao, J. M. Feinberg, and R. E. Dunin-Borkowski (2013), Ferrimagnetic/ferroelastic domain interactions in magnetite below the Verwey transition. Part I: Electron holography and Lorentz microscopy, *Phase Transitions*, *86*, 67–87.

Manahan, M. P. (1990), Thermal expansion and conductivity of magnetite flakes taken from the Oconee-2 steam generator, *J. Mater. Sci.*, *25*, 3424–3428.

Metcalf, M., and M. Fuller (1988), A synthetic TRM induction curve for fine particles generated from domain observations, *Geophys. Res. Lett.*, *15*, 503–506, doi:10.1029/GL015i005p00503.

Muxworthy, A. R., and D. Dunlop (2002), First-order reversal curve (FORC) diagrams for pseudo-single-domain magnetites at high temperature, *Earth Planet. Sci. Lett.*, *203*, 369–382.

Muxworthy, A. R., D. J. Dunlop, and W. Williams (2003), High-temperature magnetic stability of small magnetite particles, *J. Geophys. Res.*, *108*(B5), 2281, doi:10.1029/2002JB002195.

Muxworthy, A. R., D. Krása, W. Williams, and T. P. Almeida (2014), Palaeomagnetic recording fidelity of non-ideal magnetic systems, *Geochem. Geophys. Geosyst.*, *15*, 2254–2261, doi:10.1002/2014GC005249.

Néel, L. (1949), Théorie du trainage magnétique des ferromagnétiques en grains fins avec application aux terres cuites, *Ann. Geophys.*, *5*, 99–136.

Néel, L. (1955), Some theoretical aspects of rock magnetism, *Adv. Phys.*, *4*, 191–242.

Tauxe, L. (1998), *Paleomagnetic Principles and Practice*, Kluwer Acad., Dordrecht, Netherlands.

Tauxe, L., and T. Yamazaki (2007), Paleointensities, in *Treatise on Geophysics*, *Geomagnetism*, vol. 5, edited by G. Schubert, pp. 509–564, Elsevier Ltd., Oxford, U. K.

Thomson, L. C., R. J. Enkin, and W. Williams (1994), Simulated annealing of 3-Dimensional micromagnetic structures and simulated thermoremanent magnetization, *J. Geophys. Res.*, *99*, 603–609, doi:10.1029/93JB02638.

Winklhofer, M., K. Fabian, and F. Heider (1997), Magnetic blocking temperatures of magnetite calculated with a three-dimensional micromagnetic model, *J. Geophys. Res.*, *102*, 22,695–22,709, doi:10.1029/97JB01730.